Surface-Based Supramolecular Chemistry Using Hydrogen Bonds

Anna G. Slater,[†] Luis M. A. Perdigão,[‡] Peter H. Beton,[‡] and Neil R. Champness*,[†]

[†]School of Chemistry, [‡]School of Physics and Astronomy, University of Nottingham, Nottingham NG7 2RD, United Kingdom

CONSPECTUS: The arrangement of molecular species into extended structures remains the focus of much current chemical science. The organization of molecules on surfaces using intermolecular interactions has been studied to a lesser degree than solution or solid-state systems, and unanticipated observations still lie in store. Intermolecular hydrogen bonds are an attractive tool that can be used to facilitate the self-assembly of an extended structure through the careful design of target building blocks.

Our studies have focused on the use of 3,4,9,10-perylene tetracarboxylic acid diimides (PTCDIs), and related functionalized analogues, to prepare extended arrays on surfaces. These molecules are ideal for such studies because they are specifically designed to interact with appropriate diaminopyridine-functionalized molecules, and related species, through complementary hydrogen bonds. Additionally, PTCDI species can be functionalized in the bay region of the molecule, facilitating modification of the self-assembled structures that can be prepared. Through a combination of PTCDI derivatives, sometimes in combination with melamine, porous two-dimensional arrays can be formed that can entrap guest molecules. The factors that govern the self-assembly processes of PTCDI derivatives are discussed, and the ability to construct suitable target arrays and host-specific molecular species, including fullerenes and transition metal clusters, is demonstrated.
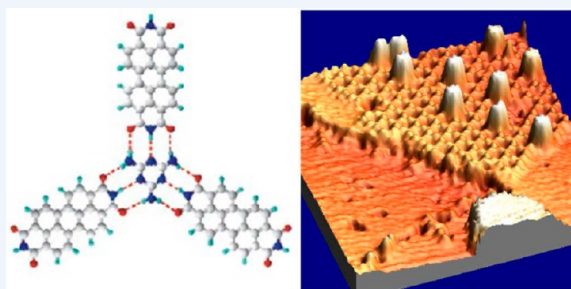
INTRODUCTION

Self-assembly has been identified as one of the most significant challenges facing science.[1−3] Indeed, the exploitation of intermolecular interactions to control the organization of molecules into nanoscale architectures has led to many fascinating systems; however, it remains clear that there are still many challenges ahead. Much of this chemistry has been performed in either the solution or solid-state phase, typically leading to discrete supramolecular architectures[4] or three-dimensional arrangements in crystalline structures.[5]

Surface-based supramolecular chemistry is an area of research that has grown extensively over recent years.[6−12] Although surface chemistry has long been used to assemble arrays of molecules, such as self-assembled monolayers (SAMs) of thiolate molecules adsorbed onto Au(111) substrates,[13] much of this chemistry relies upon van der Waals interactions and simple geometric preferences rather than stronger, well-defined supramolecular interactions. More recent studies have developed the concept of exploiting supramolecular inter-actions,[14−28] including coordination bonds,[16,17] halogen bonds,[18,19] and, notably, hydrogen bonding,[12,20−28] to control molecular organization on surfaces. Such structures can be characterized using scanning probe microscopies and partic-ularly scanning tunnelling microscopy (STM), which facilitates the identification of individual molecules and hence the arrangement of self-assembled arrays. A key feature of these studies that differs from solution phase or solid-state supra-molecular chemistry is, of course, the surface, which can have a considerable influence upon the pathway of self-assembly processes.

Early studies of hydrogen-bonded systems focused on the use of molecules that are able to form self-complementary intermolecular hydrogen bonds to produce one- or two-dimensional arrays with other molecules of the same kind.[11,12,20−29] Subsequently, a range of systems have been studied, with particular success stemming from the use of molecules containing carboxylic acid moieties,[11,21−28] which are well-known for forming robust and complementary hydrogen-bonding interactions.

A focus of our studies has been the exploitation of the strong triple-hydrogen-bonding interactions observed between imide moieties and melamine, a strategy that has allowed the development of a range of nanoscale surface-based architectures that can be prepared either in an ultrahigh vacuum or in a solution environment. Our approach has relied primarily on the use of 3,4,9,10-perylene tetracarboxylic acid diimides (PTCDIs), and related functionalized analogues, or smaller imide-containing species such as 1,4,5,8-naphthalenetetracar-boxylic diimide (NTCDI) or cyanuric acid (CA). The combination and adaptability of diimide species has allowed detailed investigations of the self-assembled structures in combination with melamine and, in addition, may form supramolecular structures formed by hydrogen bonding between the diimide species themselves. This account outlines our progress in this field, demonstrating the versatility of our approach and the potential use of such structures as templates for guest molecules.
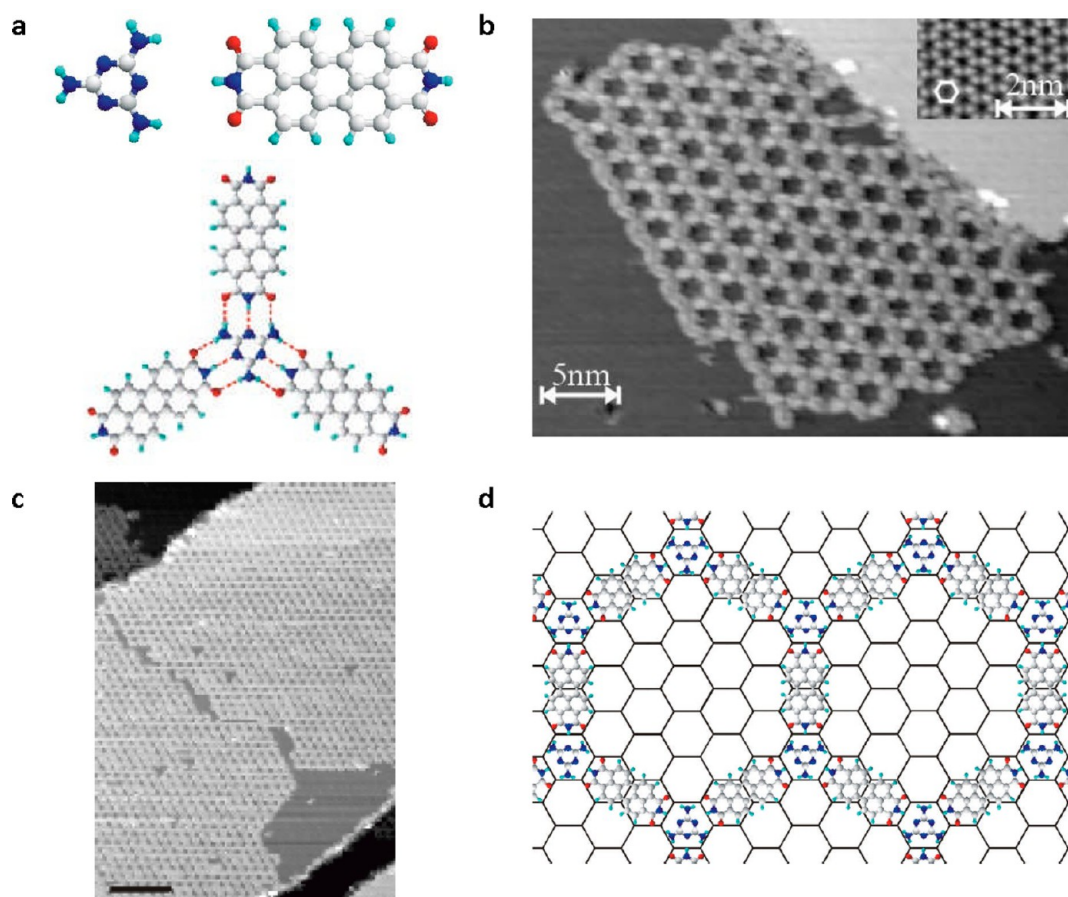
Figure 1. Self-assembly of a PTCDI−melamine supramolecular network. (a) Chemical structures of PTCDI and melamine and a representation of the PTCDI−melamine junction. Dotted lines represent hydrogen bonds between the molecules. (b) STM image of a PTCDI−melamine network. (Inset) High-resolution view of the Ag/Si(111) substrate surface. (c) STM image of large-area network, with domains extending across terraces on the Ag/Si(111) surface. Scale bar, 20 nm. (d) Schematic diagram showing the registry of the network with the Ag/Si(111) surface. For panels c and d, STM imaging parameters were as follows: sample voltage, −2 V; tunnel current, 0.1 nA. Reprinted with permission from ref 30. Copyright 2003 Nature Publishing Group.

■ THE PTCDI−MELAMINE NETWORK AND RELATED SYSTEMS

Our initial study demonstrated that PTCDI, a linear diimide molecule, interacts with melamine, which presents 3-fold hydrogen-bonding symmetry, to give rise to a honeycomb structure on a Ag−Si(111) $\sqrt{3} \times \sqrt{3}$R30° surface [named Ag/Si(111) from here on] under ultrahigh vacuum (UHV) conditions (Figure 1).[30] The Ag/Si(111) surface, while perhaps unfamiliar, is a useful surface to study self-assembly processes due to the relatively weak adsorbate−surface interaction, which allows molecular mobility and thus self-assembly. The formation of the honeycomb network was achieved by the sequential deposition of PTCDI and melamine, followed by an annealing step at ∼100 °C. The annealing step is required to form the honeycomb array, providing sufficient thermal energy for molecules to detach from PTCDI islands, diffuse across the surface, and interact with melamine molecules, resulting in the formation of the target network structure. Gas-phase DFT calculations indicate an energy of 0.73 eV/junction of three hydrogen bonds of the PTCDI···melamine interaction, significantly greater than values for two hydrogen-bond interactions between two PTCDI molecules (0.51 eV) or two melamine molecules (0.44 eV) and supporting the observation that the bimolecular PTCDI−melamine array is favored over unimolecular PTCDI or melamine arrays.

The network was found to be commensurate with the underlying Ag/Si(111) surface, indicating an influence from the substrate in the formation of the network. The resulting structure contains hexagonal pores of ca. 2.5 nm diameter, providing chemical differentiation across the surface and opening the possibility of using such structures to act as hosts to trap guest molecules, a concept discussed further below. Our relatively simple approach, using well-understood hydrogen-bonding synthons, demonstrated that the great wealth of understanding of solution-phase supramolecular chemistry could be used to inspire surface-based self-assembly.

The PTCDI−melamine network observed on Ag/Si(111)[30] can similarly be prepared on a Au(111) surface[31] using a similar preparative approach, leading to a honeycomb arrangement (Figure 2). However, unlike studies on Ag/Si(111), an additional intermixed PTCDI−melamine phase is observed prior to formation of the honeycomb array on a Au(111) substrate. Thus, deposition of melamine onto close-packed PTCDI islands[31] results in the formation of large ordered arrays of melamine molecules within which isolated PTCDI molecules, or larger aggregate rows of PTCDI molecules, are embedded. Heating this intermixed phase at ca. 50 °C results in the formation of a further phase in which chiral melamine islands are surrounded by PTCDI molecules (Figure 2a). It should be noted that at this temperature the PTCDI molecules
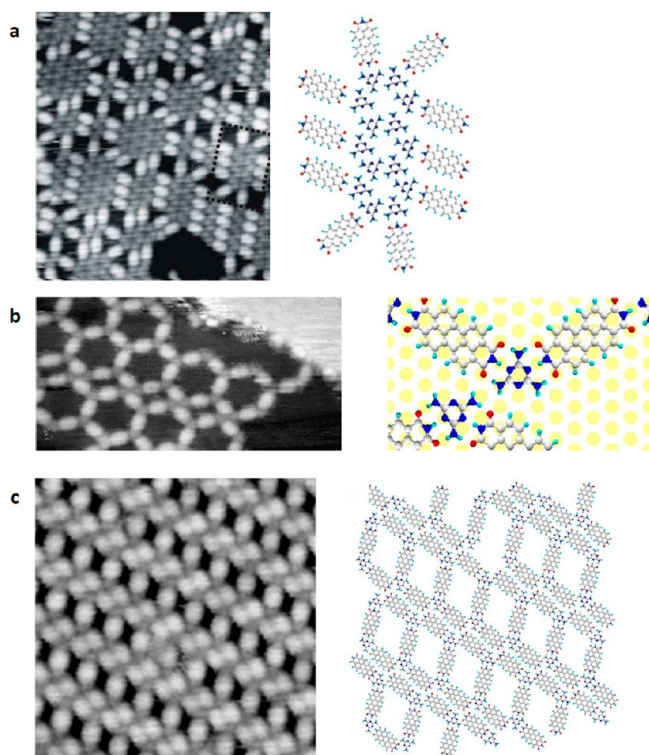
Figure 2. (a) STM image of an intermixed PTCDI−melamine phase formed on Au(111) after annealing at ∼50 °C, showing melamine islands around which PTCDI molecules are attached through hydrogen bonding (image 19.7 × 19.7 nm^2), and schematic representation of the PTCDI attachment to the melamine array, corresponding to the region marked by dotted lines in the STM image. (b) STM image showing alternative melamine−PTCDI packing in which vertexes between four PTCDI molecules are formed and schematic of the proposed arrangement overlaid on gold (image 19.0 × 7.5 nm^2). (c) STM image, showing the molecular arrangement of a parallelogram network formed on Au(111) at elevated temperatures and schematic of the proposed ordering (image 17.5 × 17.5 nm^2). For panels a and b, STM imaging parameters were as follows: sample voltage, −1.8 V; tunnel current, 0.05 nA. For panel c, STM imaging parameters were as follows: sample voltage, −1.5 V; tunnel current, 0.03 nA. Panels a and b reprinted from ref 31. Copyright 2006 American Chemical Society. Panel c reprinted with permission from ref 32. Copyright 2008 WILEY-VCH Verlag GmbH & Co. KGaA, Weinheim.

adopt triple hydrogen bonds with melamine molecules on the periphery of the islands. Further annealing of the sample, in the range 60−80 °C, results in the formation of the honeycomb structure (Figure 2b) and desorption of excess melamine molecules. The structure is very similar to that observed on Ag/Si(111),[30] but, in contrast, the structures of Au(111) also show features in which adjacent hexagons are linked through melamine vertices rather than PTCDI edges (Figure 2b). This arrangement, which adopts a highly unusual hydrogen-bonding motif, leads to the formation of smaller parallelogram-shaped pores (Figure 2b).

Interestingly, further annealing of the PTCDI−melamine network on Au(111) leads to the formation of an unanticipated parallelogram phase[32] (Figure 2c). This distinct phase is formed when the honeycomb network is heated at temperatures of ca. 90 °C and has the same stoichiometric ratio as the honeycomb structure but is more densely packed. At the boundaries of the parallelogram phase, it is possible for the honeycomb array to

coexist. Once again, the pores formed within this parallelogram phase are considerably smaller than those observed in the honeycomb structure.

The effect of the adsorbate surface on the self-assembly process is evident when comparing the observed structures on Ag/Si(111) and Au(111). Indeed, surface registry, i.e., compatibility between the dimensions of the surface lattice and those of adsorbed molecules or self-assembled structures, can play a significant role in the formation of self-assembled structures. This phenomenon is demonstrated by our attempts to prepare an array analogous to the PTCDI−melamine network using 1,4,5,8-naphthalenetetracarboxylic diimide (NTCDI). The single-component assembly of NTCDI leads to the formation of one-dimensional hydrogen-bonded chains[33] (Figure 3), but the combination of NTCDI with melamine
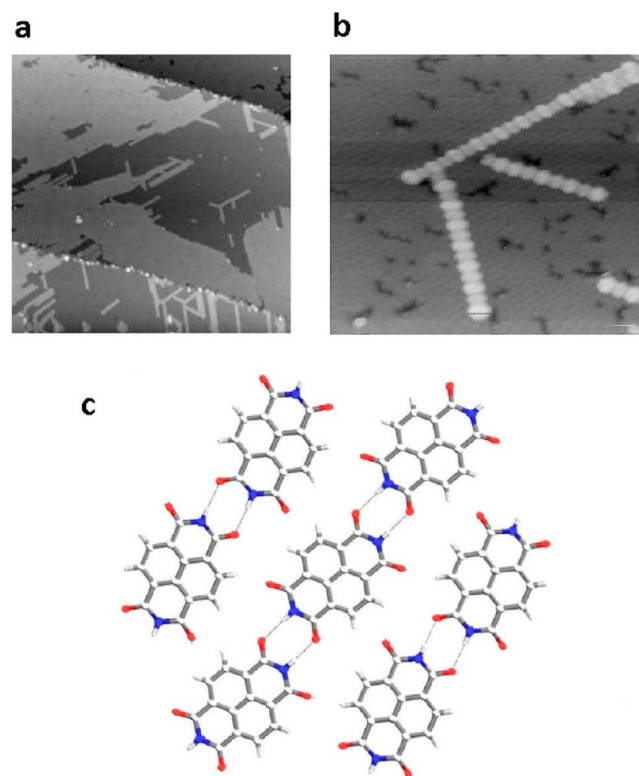

Figure 3. STM images NTCDI adsorbed on the Ag/Si(111) surface. (a) Close packed islands and single-molecule-wide chains form spontaneously at room temperature (image 150 × 150 nm^2). (b) High-resolution image of three molecular chains (c) View of hydrogen-bonded chains in the single-crystal X-ray structure of NTCDI (image 27 × 23 nm^2). Reprinted from ref 33. Copyright 2003 American Chemical Society.

does not lead to an analogous honeycomb structure on Ag/Si(111).[34] Indeed, the lack of commensurability between the hypothetical NTCDI−melamine honeycomb array and the Ag/Si(111) surface structure leads to the formation of a range of other motifs that do not form long-range networks, indicating that the self-assembly process does not have a strong preference for a single polymorph.

In contrast, melamine and cyanuric acid (CA) form a well-ordered network. CA presents three imide functional groups linked in a molecule with 3-fold symmetry, and in many ways, the CA−melamine array can be considered the parent compound to the PTCDI−melamine network described

above. Indeed, the interaction formed between CA and melamine, and derivatives of the two compounds, represents one of the most extensively studied structural motifs in supramolecular chemistry.[35] The CA–melamine network can be formed under ultrahigh vacuum (UHV) conditions on either a Ag/Si(111)[36] or Au(111)[37] surface and imaged using STM. On both surfaces, the anticipated 1:1 CA–melamine network is observed, but on Au(111), an alternative superstructure is also formed, consisting of a regular array of chiral hexagonal rings of melamine, linked by single molecules of cyanuric acid, reinforcing the effects that the adsorbate surface can have on the observed self-assembled structure.

■ FUNCTIONALIZED PTCDI SELF-ASSEMBLED ARRAYS

One of the advantages of using PTCDI as a building block in forming self-assembled structures is the rich chemistry that has been developed surrounding such molecules.[38] We have developed a series of PTCDI molecules that are substituted in what is known as the "bay region" of the molecule. Through bromination of the bay-region of N-alkylated PTCDI species, it is possible to introduce a variety of functional groups[39–42] (Scheme 1), allowing the formation of functionalized PTCDI building blocks through the conversion of the N-alkylated imide to N–H functionalized imides. These building blocks can

Scheme 1. PTCDI and Related Derivatives Discussed in This Account[a]
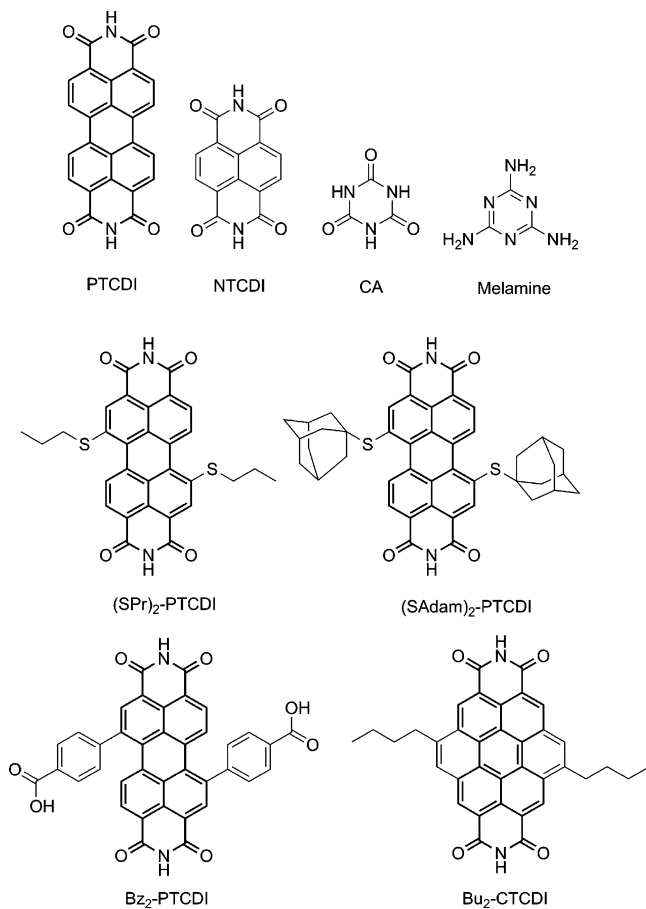
[a]Note the variation in functionalization of the bay region of the PTCDI derivatives.

be used for the formation of self-assembled structures and have been studied on Ag/Si(111),[39,41] Au(111),[42] and, more recently, graphene[40] surfaces.

An attractive target are S-functionalized species such as (SPr)$_2$–PTCDI (Scheme 1). The target molecule can be readily synthesized through substitution of dibromo-functionalized PTCDI with propanethiolate. Intriguingly, deposition of (SPr)$_2$–PTCDI onto Ag/Si(111) in UHV and subsequent imaging by STM reveals the formation of a hydrogen-bonded honeycomb structure by (SPr)$_2$–PTCDI even in the absence of melamine (Figure 4).[39] The structure is formed through the
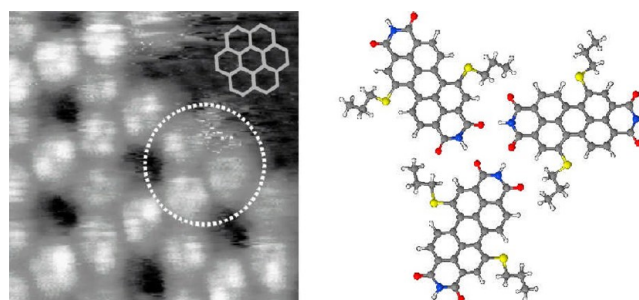

Figure 4. View of an STM image of a hexagonal region of (SPr)$_2$–PTCDI on Ag/Si(111) (image 8 × 8 nm^2) and schematic representation of the hydrogen-bonded trimer node (highlighted in the STM image with a dashed white circle) and the surface reconstruction represented with a hexagonal mesh. For panel a, the STM imaging parameters were as follows: sample voltage, −2.5 V; tunnel current, 0.03 nA. Reprinted with permission from ref 39. Copyright 2008 WILEY-VCH Verlag GmbH & Co. KGaA, Weinheim.

adoption of hydrogen-bonded vertices at the junction of three molecules and stabilized by three hydrogen bonds between the N–H groups on one molecule and one of the C=O groups on a neighboring molecule. This triple vertex hydrogen-bonding configuration is similar to the stabilizing linkage proposed for cyanuric acid on the same surface[36] and is chiral. The formation of a two-dimensional network by (SPr)$_2$–PTCDI on Ag/Si(111) contrasts with the behavior of Br$_2$–PTCDI, which has a greater tendency to form simple one-dimensional hydrogen-bonded chains under the same conditions.[39] The relative stabilization of the triple vertex for (SPr)$_2$–PTCDI, in comparison to the dimeric arrangement observed for Br$_2$–PTCDI, is supported by gas-phase DFT calculations[39] that indicate that an energy of 0.86 eV is observed for a configuration in which imide carbonyl groups interact with propylthio chains from adjacent molecules through C–H···O hydrogen bonds (see Figure 4 for arrangement). In both instances, codeposition of melamine with either (SPr)$_2$–PTCDI or Br$_2$–PTCDI on Ag/Si(111) leads to the formation of the anticipated functionalized PTCDI–melamine bimolecular array, mimicking the prototypical network discussed above.

We have also compared the self-assembly processes of (SPr)$_2$–PTCDI, PTCDI, and 1,7-di(butyl)-coronene-3,4:9,10-tetracarboxylic acid diimide (Bu$_2$–CTCDI) on a graphene-terminated metal substrate.[40] The graphene monolayer is grown on a Rh(111) crystal, and, consequently, the surface exhibits a moiré pattern, introducing distinct adsorption sites on the surface and therefore offering the possibility that the surface will significantly influence the self-assembly process. For the three diimide molecules studied, PTCDI, (SPr)$_2$–PTCDI, and Bu$_2$–CTCDI, two distinct types of arrays are observed involving distinct junctions formed by either two or three
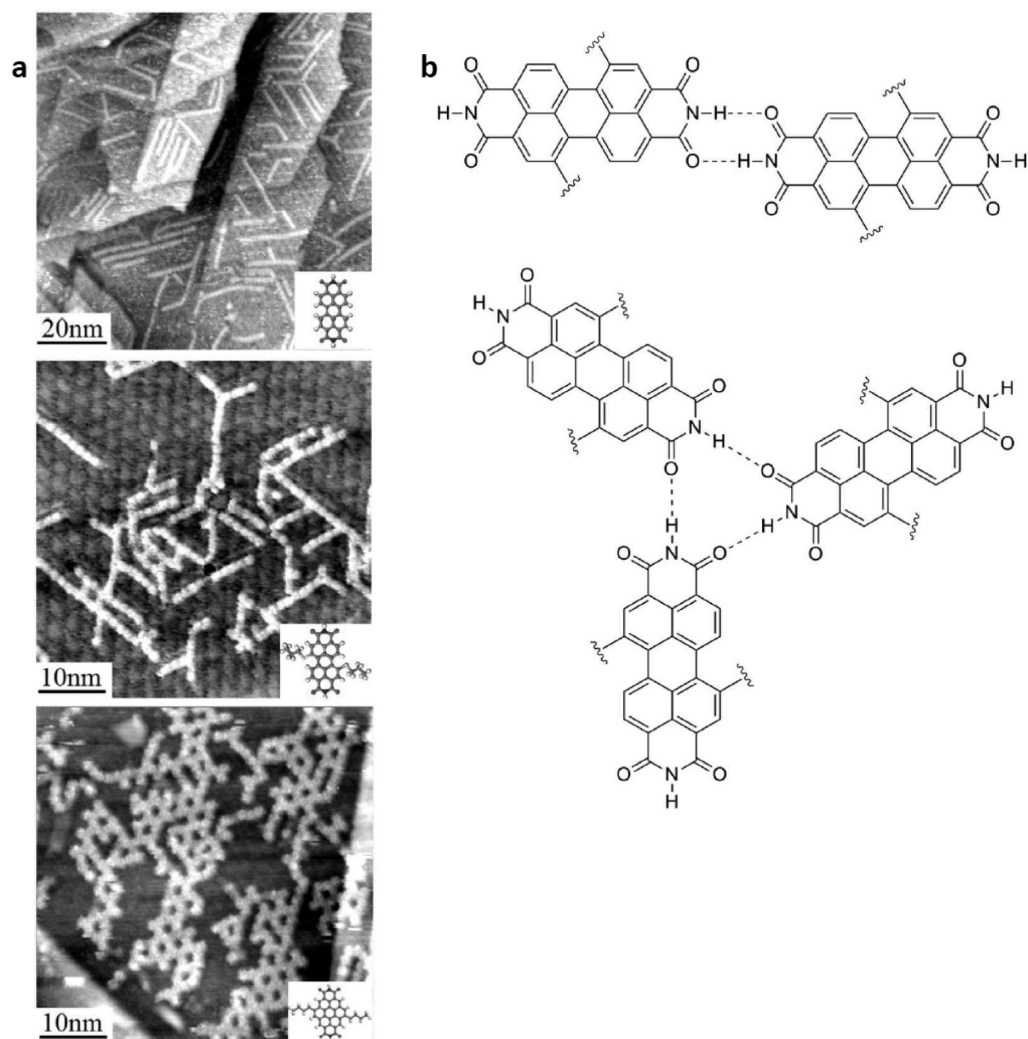
Figure 5. (a) STM images of PTCDI (top), (SPr)$_2$−PTCDI (middle), and Bu$_2$−CTCDI (bottom) deposited on a graphene monolayer formed on Rh(111)/YSZ/Si(111). (b) Schematic of dimeric and trimeric hydrogen-bonding junctions observed. STM imaging parameters: (a) Top image: sample voltage, −1 V; tunnel current, 0.2 nA. Middle image: sample voltage, −1 V; tunnel current, 0.1 nA. Bottom image: sample voltage, 1 V; tunnel current, 0.1 nA. Panel a reprinted with permission from ref 40. Copyright 2010 WILEY-VCH Verlag GmbH & Co. KGaA, Weinheim.

diimide molecules (Figure 5). Unfunctionalized PTCDI forms one-dimensional rows up to 25 nm in length through the adoption of simple dimeric hydrogen-bonding interactions. The formation of PTCDI chains on the graphene surface differs markedly from PTCDI structures observed on a graphite substrate, which does not exhibit a moiré pattern, on which close-packed three-dimensional islands are formed.[43] Comparison of the behavior of PTCDI on graphene to the adsorption of the same molecule on a BN "nanomesh" monolayer, which also exhibits a moiré pattern but of different periodicity to that shown by graphene on Rh(111), reveals the importance of commensurability between the molecular dimensions and the moiré periodicity of the surface. As the BN monolayer displays a moiré pattern, but with a slightly larger periodicity (3.2 nm) than that of graphene and not commensurate with the dimensions of PTCDI, isolated PTCDI molecules are trapped in energy minima associated with the moiré pattern, and no extended hydrogen-bonded structures are observed.

As with PTCDI, adsorption of (SPr)$_2$−PTCDI on graphene leads to the formation of hydrogen-bonded rows, but, compared to PTCDI, there are fewer examples of pairs of parallel rows, and many more 3-fold hydrogen-bonded

junctions are observed. Indeed, the ratio of dimer/trimer junctions is 75:25 for (SPr)$_2$−PTCDI, in contrast to less than 1% of junctions being trimers for PTCDI. Further expansion of the core of the diimide molecule in the coronene-3,4:9,10-tetracarboxylic acid diimide species Bu$_2$−CTCDI leads to domination of the self-assembly process by 3-fold junctions, with no linear dimers being unambiguously identified. The dominance of trimer formation results in a honeycomb network aligned with the graphene superstructure and enclosing areas of bright contrast arising from the moiré pattern. The formation of a honeycomb structure by Bu$_2$−CTCDI on graphene mimics the extended hydrogen-bonded structure adopted by (SPr)$_2$−PTCDI on Ag/Si(111)[39] (see above). The greater preference for forming trimer junctions in (SPr)$_2$−PTCDI and Bu$_2$−CTCDI is indicative that trimeric hydrogen-bonded arrangements are stabilized by greater steric bulk in the bay region of the diimide molecules and is supported by gas-phase DFT calculations that indicate a relative stability of the trimeric arrangement over dimeric arrangement of 0.06 eV per molecule for unfunctionalized PTCDI, of 0.11 eV for (SPr)$_2$−PTCDI, and 0.12 eV for Bu$_2$−CTCDI.[40]
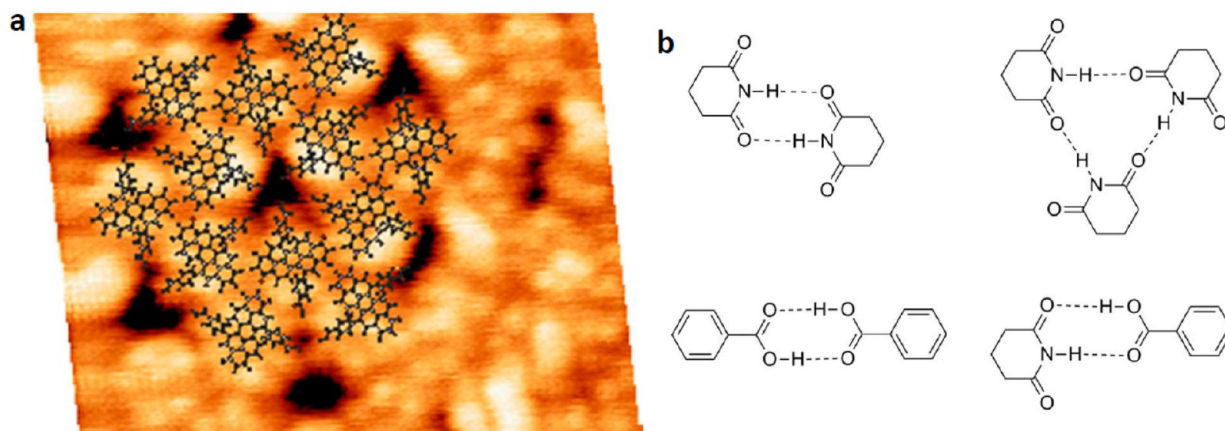

Figure 6. (a) STM image of Bz$_2$−PTCDI forming a honeycomb arrangement using the trimeric PTCDI hydrogen-bonding junction (see panel b) with overlay of molecular configuration (image 3 × 2.5 nm^2).[41] (b) Potential supramolecular synthons adopted by imides and carboxylic acids. STM imaging parameters for panel a were as follows: sample voltage, 1 V; tunnel current, 0.1 nA.

The PTCDI core can also be functionalized with aryl group via Suzuki coupling between an appropriate aryl boronic acid and N-alkylated Br$_2$−PTCDI derivatives.[41] We synthesized a PTCDI derivative, 1,7-bis(4-benzoic acid)-PTCDI (Bz$_2$− PTCDI), that was difunctionalized in the bay region by arylcarboxylic acid groups. The introduction of carboxylic acid functionality offers the potential for competition between different hydrogen-bonding moieties such that three types of interaction could potentially be adopted during a self-assembly process: imide···imide, carboxylic acid···carboxylic acid, and imide···carboxylic acid (Figure 6). The interplay of different supramolecular interactions is a critical subject in understanding self-assembly processes.[35] Gas-phase DFT calculations indicate that the carboxylic acid···carboxylic acid interactions would be anticipated to be the most stable supramolecular synthon, but this motif is only slightly more energetically favorable than the hydrogen-bonding interaction observed between three imide moieties (Figure 6), such as that observed for (SPr)$_2$−PTCDI on Ag/Si(111)[39] or Bu$_2$−CTCDI on graphene.[40] STM studies of the self-assembled structures formed by Bz$_2$−PTCDI on Ag/ Si(111)[41] reveal that of all of the possible hydrogen-bonding interactions the triple imide interactions is favored (Figure 6). Such a structure leaves the carboxylic acid groups protruding into the pores formed by the honeycomb network.

Although our initial studies were all performed in UHV conditions, a report by Buck et al. demonstrated that the PTCDI−melamine network can be assembled on a Au(111) surface from solution.[44] These studies have been developed using a difunctionalized PTCDI derivative, 1,7-diadamantane-thioperylene-3,4:9,10-tetracarboxylic diimide (SAd)$_2$− PTCDI.[42] Upon self-assembly on Au(111), (SAd)$_2$−PTCDI forms a one-dimensional structure, in contrast to either (SPr)$_2$−PTCDI,[39,40] Bz$_2$−PTCDI,[41] or Bu$_2$−CTCDI[40] on various substrates (see above). The one-dimensional structure seen for (SAd)$_2$−PTCDI also contrasts with that observed for Br$_2$−PTCDI[39] and NTCDI,[33] both of which form linear chain arrangements by adopting a zigzag arrangement presumably as a result of minimizing steric clashes while maximizing surface coverage and accommodating other weak intermolecular interactions. Co-deposition of (SAd)$_2$−PTCDI and melamine onto a Au(111) surface from DMF solution[42] results in the formation of the anticipated honeycomb structure, but close inspection of the STM images reveals a significant number of defects in the structure arising due to cleavage of a number of

the thioadamantyl groups from the (SAd)$_2$−PTCDI building blocks. The cleavage of these groups is encouraged both by the experimental conditions used for preparation of the sample and also by the presence of melamine. The effect of the random cleavage of the thioadamantyl groups through the honeycomb network is the formation of pores of different shape and size, affecting the host behavior of the (SAd)$_2$−PTCDI−melamine network (see below).

■ GUEST ENTRAPMENT IN PTCDI-BASED NETWORKS

Two-dimensional networks formed by PTCDI derivatives, both with and without melamine, contain pores (or wells) within their structures, making them ideal candidates to act as hosts for guest species. We[30−32,42,44−47] and others[48,49] have studied the behavior of such systems to trap a variety of molecular species from fullerenes to metal clusters, indicating the versatility of such an approach.

Fullerenes have provided a useful tool to probe the host−guest properties of PTCDI-based networks. Studies of the prototypical structures formed by unfunctionalized PTCDI and melamine reveal a simple relationship between pore dimensions and fullerene guest inclusion.[30] Thus, the honeycomb structure formed by PTCDI and melamine on Ag/Si(111) acts as a host for C$_{60}$ molecules hosting seven in each pore (Figure 7a). The PTCDI−melamine array on Au(111) forms different types of pores, depending on the arrangement of the hydrogen-bonded structure prepared.[31,32] Pores within the honeycomb structure are also capable of accommodating heptameric C$_{60}$ clusters, but, interestingly, the same pores also accommodate hexameric C$_{60}$ clusters (Figure 7b) in which the central fullerene molecule is missing.[32] This behavior is accounted for by a small increase in pore dimensions on the Au(111) substrate, resulting in a reduced entrapment strength for the C$_{60}$ heptamer. The PTCDI−melamine honeycomb network on Au(111) forms in combination with smaller pores that can host just two C$_{60}$ molecules (Figure 7b).

We have also studied the ability of the PTCDI−melamine honeycomb network, on Ag/Si(111), to host the larger fullerene C$_{84}$.[45] In contrast to the studies of C$_{60}$, adsorption of C$_{84}$ onto the network leads to the formation of a range of smaller clusters in addition to the heptameric fullerene assembly. Indeed, clusters ranging from dimers to heptamers
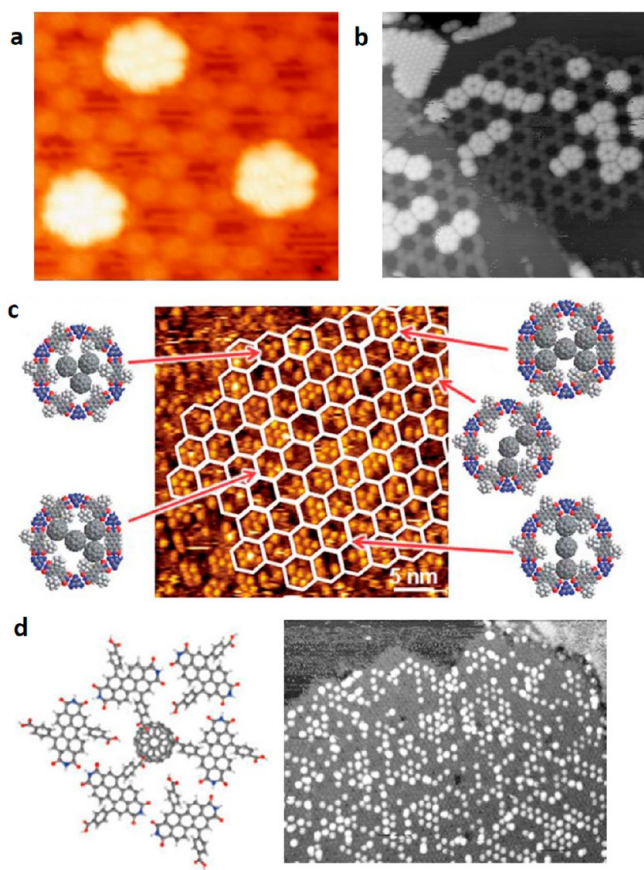
Figure 7. Images of C_{60} molecules trapped within hydrogen-bonded hosts. (a) C_{60} heptamers trapped within the PTCDI−melamine array on Ag/Si(111) (image 7 × 6 nm²).[30] (b) C_{60} clusters, predominantly hexamers, captured in pores of the PTCDI−melamine network on Au(111) (image 3.94 × 3.94 nm²).[31] (c) C_{60} entrapment in a (SAdam)$_2$−PTCDI−melamine network on Au(111); the honeycomb network is indicated as a guide to the eye. Schematic figures illustrate and identify the different arrangements of C_{60} within the pores of the structure that arise due to missing adamantyl units.[42] (d) Proposed model for encapsulation of individual C_{60} molecules within the pores of Bz$_2$−PTCDI and an STM image showing single C_{60} entrapment onto the molecular cavities (image 10 × 8 nm²).[41] STM imaging parameters were as follows: (a) sample voltage, −2 V; tunnel current, 0.1 nA; (b) sample voltage, −2 V; tunnel current, 0.05 nA; (c) sample voltage, −0.34 V; tunnel current, 0.028 nA; (d) sample voltage, 1.1 V; tunnel current, 0.03 nA. Panel a reprinted with permission from ref 30. Copyright 2003 Nature Publishing Group. Panel b reprinted from ref 31. Copyright 2006 American Chemical Society. Panel c reprinted with permission from ref 42. Copyright 2010 Royal Society of Chemistry. Panel d reprinted with permission from ref 41. Copyright 2010 Royal Society of Chemistry.

are observed. Statistical analysis of the observed fullerene clusters indicates that the orientation of the cluster can switch when the size of the cluster increases by addition of a single molecule. Thus, unlike the corresponding studies of C_{60} entrapment by the PTCDI−melamine network, studies of C_{84} reveal a stepwise formation of the molecular clusters trapped within the honeycomb pores.

The network formed by unfunctionalized PTCDI and melamine on Au(111) at elevated temperatures, ca. 90 °C, encloses parallelogram-shaped pores that are of sufficient dimensions to accommodate two C_{60} molecules.[32] Interestingly, analysis of STM images of this parallelogram network

hosting C_{60} molecules reveals an enhanced probability for occupation of neighboring pores along a row of pores. The nonrandom organization of fullerene dimers within the network provides clear evidence of a hierarchy of organization within this system. Similar studies by Silly et al. have demonstrated entrapment of Lu@C_{82} by the PTCDI−melamine parallelogram network.[46]

Functionalization of the PTCDI molecule can be used to modify the entrapment properties of the self-assembled frameworks. Thus, honeycomb networks formed between melamine and PTCDI derivatives, or in some instances networks formed by the PTCDI derivatives alone, can act as hosts to guest fullerene molecules. The honeycomb array formed by Br$_2$−PTCDI and melamine on Ag/Si(111) will accommodate C_{60} heptamers in an analogous fashion to that of the parent unfunctionalized PTCDI−melamine array.[39] In contrast, functionalization of the PTCDI species with the sterically larger thiopropyl groups in (SPr)$_2$−PTCDI results in very different adsorption behavior.[39] The (SPr)$_2$−PTCDI−melamine array does not trap heptamers or hexamers, in contrast to that for PTCDI and Br$_2$−PTCDI analogues. Although some fullerenes can be observed in STM images, these are positioned in an irregular fashion both within pores and also on top of the honeycomb array. These images indicate that the thiopropyl groups act to inhibit fullerene adsorption by this network.

The network formed by thioadamantyl functionalized PTCDI, (SAdam)$_2$−PTCDI, and melamine exhibits a honeycomb structure.[42] It should be noted that the thioadmantyl group is considerably more bulky than the thiopropyl appendages of (SPr)$_2$−PTCDI and importantly the adamantyl groups are more rigid, potentially providing an effective mechanism for blocking defined areas of the pores formed with the honeycomb network. However, as discussed above, some of the thioadamantyl groups are cleaved from the PTCDI moieties upon formation of the (SAdam)$_2$−PTCDI−melamine network.[42] As a result, a series of pores of distinct size and configuration are formed by the network. Adsorption of C_{60} by the network facilitates visualization of the different pores. STM imaging following C_{60} entrapment allows identification of individual fullerene molecules and precise identification of the different orientations of the molecular clusters within each pore (Figure 7c). The number of C_{60} molecules adsorbed within a given pore is determined by the degree of thioadamantyl cleavage, and clusters ranging from dimers to heptamers are observed. Considering the dimensions of the honeycomb pores and the size of the thioadamantyl appendages, clusters of greater than five fullerenes can be explained only by cleavage of the thioadamantyl groups. The adsorption of C_{60} within the (SAdam)$_2$−PTCDI−melamine network also depends on the relative orientation of the thioadamantyl groups that protrude into the pore. There are two possible orientations of the adamantyl units, as they are located on a σ_2 mirror axis of the molecule, and as a result it is possible that adjacent adamantyl groups around the periphery of the pore are positioned either in close proximity or separated by a gap sufficient to accommodate a guest C_{60} molecule.

Further constriction of pore size can be used to control the number of guest fullerene molecules. This principal is demonstrated by the Bz$_2$−PTCDI hydrogen-bonded framework. The assembly of a honeycomb array by solely Bz$_2$−PTCDI coupled with the rigid protrusion of phenylcarboxylate moieties into the framework cavities allows the encapsulation of

a single C_{60} molecule, which is spaced in a regular fashion across the surface (Figure 7d).

It is also possible to entrap alkanethiol molecules within the pores of the networks formed by PTCDI and its derivatives. Buck et al. demonstrated the entrapment of adamantanethiol, ω-(4′-methylbiphenyl-4-yl)propanethiol, or dodecanethiol within the pores of the PTCDI−melamine array on a Au(111) surface.[44] Indeed, introduction of guest thiol molecules into the pores of the network is readily achieved through immersion of the hydrogen-bonded array into solutions of the target thiol. Adamantanethiol has also been used to probe the nature of networks formed by $(SAdam)_2$−PTCDI−melamine under solution, providing a mechanism for probing the degree and arrangement of cleavage of thioadamantyl appendages from the hydrogen-bonded network (see above).[42] We have also investigated the entrapment of dodecanethiol molecules in the PTCDI−melamine parallelogram network (see above) on Au(111) but under UHV conditions.[45] In contrast to studies where the alkanethiol is introduced from solution, sublimation of the dodecanethiol onto the PTCDI−melamine network in UHV leads to the thiol molecules sitting parallel, rather than perpendicular, to the surface. As a result, the pore volume accommodates fewer thiol molecules, and in the case of dodecanethiol, only two molecules can be accommodated per pore. It is interesting to note that adsorption of dodecanethiol onto the PTCDI−melamine arrays lead to the destruction of the honeycomb phase but not the parallelogram phase, suggesting that the latter is preferentially stabilized by the thiol guest.[45]

The introduction of more complex molecules onto hydrogen-bonded arrays requires appropriate, typically softer, methods of molecular deposition. This can be achieved either through solution-based methods or more recently via electrospray methodology.[48,49] We have investigated the use of the electrospray approach to deposit $Mn_{12}O_{12}(O_2CCH_3)_{16}(H_2O)_4$ clusters onto the PTCDI−melamine hydrogen-bonded array on a Au(111) substrate[49] in an attempt to control the organization of this molecule, which can act as a single-molecule magnet, in two-dimensional space. It is not possible to sublime the $Mn_{12}O_{12}(O_2CCH_3)_{16}(H_2O)_4$ cluster due to its decomposition at elevated temperatures and therefore deposition by electrospray approaches is an ideal methodology to deposit this sensitive species. In the absence of the hydrogen-bonded array, the $Mn_{12}O_{12}(O_2CCH_3)_{16}(H_2O)_4$ clusters assemble to afford filamentary structures that run over the surface (Figure 8a). When the $Mn_{12}O_{12}(O_2CCH_3)_{16}(H_2O)_4$ clusters are deposited onto the PTCDI−melamine array and although some molecules are accommodated by the pores of the hydrogen-bonded network (Figure 8b), other molecules sit on top of the array. The entrapment of the $Mn_{12}O_{12}(O_2CCH_3)_{16}(H_2O)_4$ clusters in the array is not as efficient as that of other molecules, such as fullerenes, and this is most probably due to a mismatch of dimensions between the cluster (1.6 nm) and pore (2.5 nm), diminishing favorable van der Waal's interactions between pore and guest. This clearly indicates that to achieve maximum organization of guest molecules by such porous frameworks it is important to achieve an idealized size match and to maximize interactions between host and guest.

CONCLUSIONS

Our studies have developed a clear strategy to use hydrogen bonds to create two-dimensional arrays on surfaces, mimicking strategies used by supramolecular chemists in solution and the
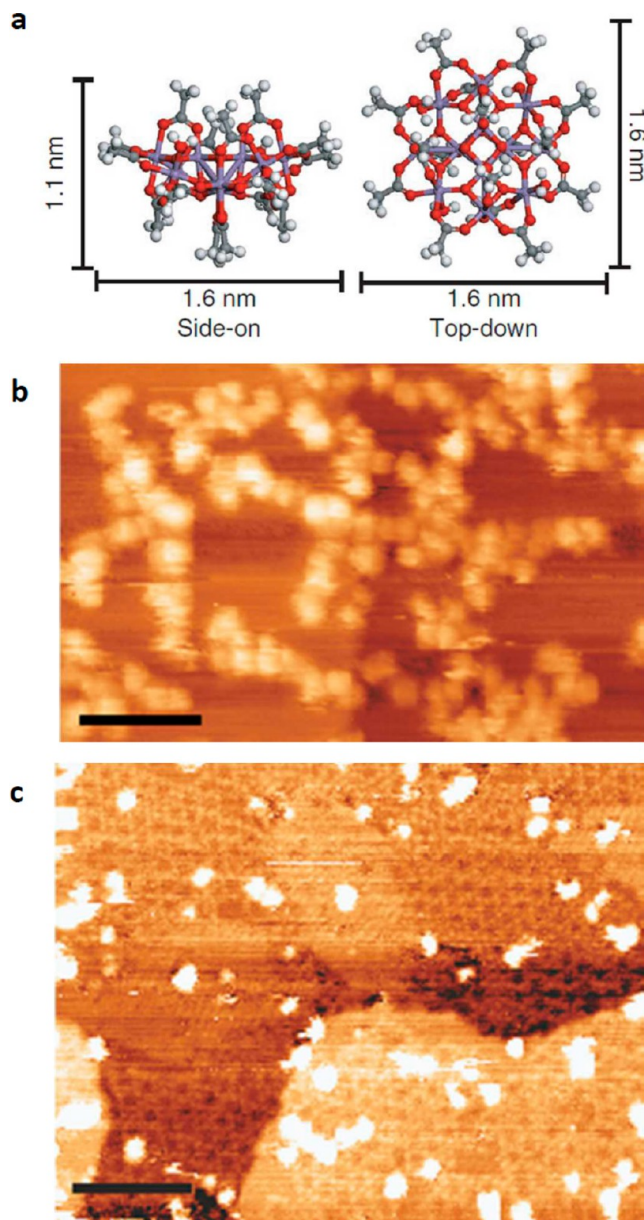

Figure 8. (a) Schematic representation of $Mn_{12}O_{12}(O_2CCH_3)_{16}(H_2O)_4$; STM images showing (b) the filamentary structures formed by molecular aggregates composed of individual $Mn_{12}O_{12}(O_2CCH_3)_{16}(H_2O)_4$ molecules. Scale bar, 10 nm. (c) $Mn_{12}O_{12}(O_2CCH_3)_{16}(H_2O)_4$ molecules deposited onto a PTCDI−melamine network on a Au(111) surface. Scale bar, 20 nm. STM imaging parameters were as follows: (b) sample voltage, +2 V; tunnel current, 0.05 nA; (c) sample voltage, +1.8 V; tunnel current, 0.03 nA. Reprinted with permission from ref 49. Copyright 2010 Nature Publishing Group.

solid state. However, clear differences are observed between self-assembly on surfaces and other environments. The surface can have a significant role to play and surface commensurability, and substrate−molecule interactions are particularly important in determining the product of a self-assembly process. Subtle variations in the dimensions of the self-assembled arrays can lead to significant effects when the framework structures are used as hosts for guest species. This is evident in the ability of the PTCDI−melamine array to template the formation of C_{60} aggregates, where the slight increase in pore dimensions observed on Au(111) in

comparison to that on Ag/Si(111) leads to a less efficient assembly of C_{60} heptamers. Where there is a significant mismatch between pore and guest dimensions, the process of trapping guest molecules becomes less efficient, illustrating the need for better control over pore dimensions. We have illustrated that it is possible to manipulate the dimensions of framework pores through functionalization of the PTCDI moiety in the molecule's bay region. This approach not only leads to variation of the pores in PTCDI−melamine arrays but also facilitates the formation of homomolecular arrays based on the functionalized PTCDI species, via adoption of trimeric hydrogen-bonded vertices.

Our studies have also revealed that surface-based self-assembly can differ significantly from solution-phase or solid-state processes. In part, this is due to the role of the surface in influencing the self-assembled structures, but it is also clear that subtle energetic balances between different arrangements can lead to multiple self-assembled phases. Minor phases can easily be overlooked by spectroscopic and diffraction techniques used for solution or solid-state systems. In contrast, characterization by STM readily reveals the variety of structures that can be formed by the self-assembly of molecules that interact through weak intermolecular interactions. The breadth of polymorphic arrangements indicates that the self-assembled structures are not necessarily the lowest energy arrangements, rather entropic factors can play a vital role in determining the structures that are formed.[25] We anticipate that theoretical investigations will play an increasingly important role, in partnership with experimental studies, in determining the best methods of creating surface-based self-assembled structures. The influence of kinetics over the structures and arrangements of self-assembled structures provides a major challenge in terms of preparing predictable structures but also opens up the possibility for highly unusual structures, including arrangements without translational periodicity[25] and quasicrystalline arrangements.[50] However, for applications where ordering is beneficial, such as magnetic systems,[49] the lack of predictability and long-range order still pose major challenges.

In summary, our approach allows the formation of two-dimensional self-assembled arrays on surfaces whose structure can be readily manipulated and modified by judicious chemical modification of component molecules. The entrapment of guest molecules with specific functionality opens up the possibility of using such arrays for organizing chemical and physical properties on the molecular scale.

■ AUTHOR INFORMATION

Corresponding Author

*E-mail: Neil.Champness@nottingham.ac.uk.

Notes

The authors declare no competing financial interest.

Biographies

Anna G. Slater is currently a Postdoctoral Research Associate working in Materials Chemistry in the group of Professor Andy Cooper at the University of Liverpool. She obtained her Ph.D. from the University of Nottingham, where she worked on the synthesis of perylene bisimide derivatives for surface self-assembly in the group of Professor Neil Champness. Her research interests include the study of complex mixtures, high-throughput screening and flow chemistry, self-assembly, synthesis optimization, and dynamic combinatorial chemistry.

Luis M. A. Perdigão is currently a Researcher at the Department of Chemistry, University of Warwick, having previously worked at the School of Physics, University of Nottingham. His interests are in the fields of nanoscience and scanning tunneling microscopy of molecules, focusing on the technical aspects of imaging and deposition and specializing in the characterization and accurate measurement of molecular structures.

Peter H. Beton is Professor of Physics at the University of Nottingham. His research interests include studies of molecules adsorbed on surfaces, particularly using scanning probe microscopies, and how such molecules can be induced to form structures with novel optical and electronic properties.

Neil R. Champness is Professor of Chemical Nanoscience and Head of Inorganic and Materials Chemistry at the University of Nottingham. His research interests include chemical nanoscience and all aspects of molecular organization, including surface supramolecular assembly and organization in the solid state via crystal engineering.

■ ACKNOWLEDGMENTS

■ REFERENCES

(1) Service, R. F. How Far Can We Push Chemical Self-Assembly? *Science* **2005**, *309*, 95.

(2) Lehn, J.-M. Toward Complex Matter: Supramolecular Chemistry and Self-Organization. *Proc. Natl. Acad. Sci. U.S.A.* **2002**, *99*, 4763−4768.

(3) Whitesides, G. M.; Boncheva, M. Beyond Molecules: Self-Assembly of Mesoscopic and Macroscopic Components. *Proc. Natl. Acad. Sci. U.S.A.* **2002**, *99*, 4769−4774.

(4) Cantrill, S. J.; Chichak, K. S.; Peters, A. J.; Stoddart, J. F. Nanoscale Borromean Rings. *Acc. Chem. Res.* **2005**, *38*, 1−9.

(5) Zhao, D.; Timmons, D. J.; Yuan, D.; Zhou, H.-C. Tuning the Topology and Functionality of Metal−Organic Frameworks by Ligand Design. *Acc. Chem. Res.* **2011**, *44*, 123−133.

(6) Slater (née Phillips), A. G.; Beton, P. H.; Champness, N. R. Two-Dimensional Supramolecular Chemistry on Surfaces. *Chem. Sci.* **2011**, *2*, 1440−1448.

(7) Elemans, J. A. A. W.; Lei, S.; De Feyter, S. Molecular and Supramolecular Networks on Surfaces: From Two-Dimensional Crystal Engineering to Reactivity. *Angew. Chem., Int. Ed.* **2009**, *48*, 7298−7332.

(8) Cicoira, F.; Santato, C.; Rosei, F. Two-Dimensional Nano-templates as Surface Cues for the Controlled Assembly of Organic Molecules. *Top. Curr. Chem.* **2008**, *285*, 203−267.

(9) Bartels, L. Tailoring Molecular Layers at Metal Surfaces. *Nat. Chem.* **2010**, *2*, 87−95.

(10) Barth, J. V.; Costantini, G.; Kern, K. Engineering Atomic and Molecular Nanostructures at Surfaces. *Nature* **2005**, *437*, 671−679.

(11) De Feyter, S.; Gesquière, A.; Abdel-Mottaleb, M. M.; Grim, P. C. M.; De Schryver, F. C.; Meiners, C.; Sieffert, M.; Valiyaveettil, S.; Müllen, K. Scanning Tunneling Microscopy: A Unique Tool in the Study of Chirality, Dynamics, and Reactivity in Physisorbed Organic Monolayers. *Acc. Chem. Res.* **2000**, *33*, 520−531.

(12) Plass, K. E.; Grzesiak, A. L.; Matzger, A. J. Molecular Packing and Symmetry of Two-Dimensional Crystals. *Acc. Chem. Res.* **2007**, *40*, 287−293.

(13) Vericat, C.; Vela, M. E.; Benitez, G.; Carro, P.; Salvarezza, R. C. Self-Assembled Monolayers of Thiols and Dithiols on Gold: New Challenges for a Well-Known System. *Chem. Soc. Rev.* **2010**, *39*, 1805−1834.

(14) Böhringer, M.; Morgenstern, K.; Schneider, W.-D.; Berndt, R. Separation of a Racemic Mixture of Two-Dimensional Molecular Clusters by Scanning Tunneling Microscopy. *Angew. Chem., Int. Ed.* **1999**, *38*, 821–823.

(15) Yokoyama, T.; Yokoyama, S.; Kamikado, T.; Okuno, Y.; Mashiko, S. Selective Assembly on a Surface of Supramolecular Aggregates with Controlled Size and Shape. *Nature* **2001**, *413*, 619–621.

(16) Stepanow, S.; Lingenfelder, M.; Dmitriev, A.; Spillmann, H.; Delvigne, E.; Lin, N.; Deng, X. B.; Cai, C. Z.; Barth, J. V.; Kern, K. Steering Molecular Organization and Host−Guest Interactions Using Two-Dimensional Nanoporous Coordination Systems. *Nat. Mater.* **2004**, *3*, 229–233.

(17) Vijayaraghavan, S.; Ecija, D.; Auwaerter, W.; Joshi, S.; Seufert, K.; Drach, M.; Nieckarz, D.; Szabelski, P.; Aurisicchio, C.; Bonifazi, D.; Barth, J. V. Supramolecular Assembly of Interfacial Nanoporous Networks with Simultaneous Expression of Metal−Organic and Organic-Bonding Motifs. *Chem.—Eur. J.* **2013**, *19*, 14143–14150.

(18) Yoon, J. K.; Son, W.-j.; Chung, K.-H.; Kim, H.; Han, S.; Kahng, S.-J. Visualizing Halogen Bonds in Planar Supramolecular Systems. *J. Phys. Chem. C* **2011**, *115*, 2297–2301.

(19) Gutzler, R.; Fu, C.; Dadvand, A.; Hua, Y.; MacLeod, J. M.; Rosei, F.; Perepichka, D. F. Halogen Bonds in 2D Supramolecular Self-Assembly of Organic Semiconductors. *Nanoscale* **2012**, *4*, 5965–5971.

(20) Barth, J. V.; Weckesser, J.; Cai, C.; Günter, P.; Bürgi, L.; Jeandupeux, O.; Kern, K. Building Supramolecular Nanostructures at Surfaces by Hydrogen Bonding. *Angew. Chem., Int. Ed.* **2000**, *39*, 1230–1234.

(21) Griessl, S.; Lackinger, M.; Edelwirth, M.; Hietschold, M.; Heckl, W. M. Self-Assembled Two-Dimensional Molecular Host−Guest Architectures From Trimesic Acid. *Single Mol.* **2002**, *3*, 25–31.

(22) Zhou, H.; Dang, H.; Yi, J.-H.; Nanci, A.; Rochefort, A.; Wuest, J. D. Frustrated 2D Molecular Crystallization. *J. Am. Chem. Soc.* **2007**, *129*, 13774–13775.

(23) Otero, R.; Schock, M.; Molina, L. M.; Laegsgaard, E.; Stensgaard, I.; Hammer, B.; Besenbacher, F. Guanine Quartet Networks Stabilized by Cooperative Hydrogen Bonds. *Angew. Chem., Int. Ed.* **2005**, *44*, 2270–2275.

(24) Li, M.; Deng, K.; Lei, S.-B.; Yang, Y.-L.; Wang, T.-S.; Shen, Y.-T.; Wang, C.; Zeng, Q.-D.; Wang, C. Site-Selective Fabrication of Two-Dimensional Fullerene Arrays by Using a Supramolecular Template at the Liquid−Solid Interface. *Angew. Chem., Int. Ed.* **2008**, *47*, 6717–6721.

(25) Blunt, M. O.; Russell, J.; Giménez-López, M. C.; Garrahan, J. P.; Lin, X.; Schröder, M.; Champness, N. R.; Beton, P. H. Random Tiling and Topological Defects in a Two-Dimensional Molecular Network. *Science* **2008**, *322*, 1077.

(26) Blunt, M. O.; Russell, J. C.; Gimenez-Lopez, M. C.; Taleb, N.; Lin, X.; Schröder, M.; Champness, N. R.; Beton, P. H. Guest-Induced Growth of a Surface-Based Supramolecular Bilayer. *Nat. Chem.* **2011**, *3*, 74–78.

(27) Stannard, A.; Russell, J. C.; Blunt, M. O.; Sallesiotis, C.; Gimenez-Lopez, M. C.; Taleb, N.; Schroder, M.; Champness, N. R.; Garrahan, J. P.; Beton, P. H. Broken Symmetry and the Variation of Critical Properties in the Phase Behaviour of Supramolecular Rhombus Tilings. *Nat. Chem.* **2012**, *4*, 112–117.

(28) Gutzler, R.; Cardenas, L.; Rosei, F. Kinetics and Thermodynamics in Surface-Confined Molecular Self-Assembly. *Chem. Sci.* **2011**, *2*, 2290–2300.

(29) Uder, B.; Ludwig, C.; Petersen, J.; Gompf, B.; Eisenmenger, W. STM Characterization of Organic Molecules on H-Terminated Si(111). *Z. Phys. B: Condens. Matter* **1995**, *97*, 389–390.

(30) Theobald, J. A.; Oxtoby, N. S.; Phillips, M. A.; Champness, N. R.; Beton, P. H. Controlling Molecular Deposition and Layer Structure with Supramolecular Surface Assemblies. *Nature* **2003**, *424*, 1029–1031.

(31) Perdigão, L. M. A.; Perkins, E. W.; Ma, J.; Staniec, P. A.; Rogers, B. L.; Champness, N. R.; Beton, P. H. Bimolecular Networks and Supramolecular Traps on Au(111). *J. Phys. Chem. B* **2006**, *110*, 12539–12542.

(32) Staniec, P. A.; Perdigão, L. M. A.; Saywell, A.; Champness, N. R.; Beton, P. H. Hierarchical Organisation on a Two Dimensional Supramolecular Network. *ChemPhysChem* **2007**, *8*, 2177–2181.

(33) Keeling, D. L.; Oxtoby, N. S.; Wilson, C.; Humphry, M. J.; Champness, N. R.; Beton, P. H. Assembly and Processing of Hydrogen-Bond Induced Supramolecular Nanostructures. *Nano Lett.* **2003**, *3*, 9–12.

(34) Perdigão, L. M. A.; Fontes, G. N.; Rogers, B. L.; Oxtoby, N. S.; Goretzki, G.; Champness, N. R.; Beton, P. H. Formation of Triangular and Row Structures of Coadsorbed NTCDI−Melamine Mixed Phases on Ag-Si(111). *Phys.Rev. B* **2007**, *76*, 245402.

(35) Whitesides, G. M.; Simanek, E. E.; Mathias, J. P.; Seto, C. T.; Chin, D. N.; Mammen, M.; Gordon, D. M. Noncovalent Synthesis: Using Physical-Organic Chemistry To Make Aggregates. *Acc. Chem. Res.* **1995**, *28*, 37–44.

(36) Perdigão, L. M. A.; Champness, N. R.; Beton, P. H. Surface Self-Assembly of the Cyanuric Acid−Melamine Hydrogen Bonded Network. *Chem. Commun.* **2006**, 538–540.

(37) Staniec, P. A.; Perdigão, L. M. A.; Rogers, B. L.; Champness, N. R.; Beton, P. H. Honeycomb Networks and Chiral Superstructures Formed by Cyanuric Acid and Melamine on Au(111). *J. Phys. Chem. C* **2007**, *111*, 886–893.

(38) Würthner, F. Perylene Bisimide Dyes As Versatile Building Blocks for Functional Supramolecular Architectures. *Chem. Commun.* **2004**, 1564–1579.

(39) Perdigão, L. M. A.; Saywell, A.; Fontes, G. N.; Staniec, P. A.; Goretzki, G.; Phillips, A. G.; Champness, N. R.; Beton, P. H. Formation of Two-Dimensional Functionalized Supramolecular Porous Nanocavity Arrays for Controlled Surface Templating. *Chem.—Eur. J.* **2008**, *14*, 7600–7607.

(40) Pollard, A. J.; Perkins, E. W.; Smith, N. A.; Saywell, A.; Goretzki, G.; Phillips, A. G.; Argent, S. P.; Sachdev, H.; Müller, F.; Hüfner, S.; Gsell, S.; Fischer, M.; Schreck, M.; Osterwalder, J.; Greber, T.; Berner, S.; Champness, N. R.; Beton, P. H. Supramolecular Assemblies Formed on an Epitaxial Graphene Superstructure. *Angew. Chem., Int. Ed.* **2010**, *49*, 1794–1799.

(41) Phillips, A. G.; Perdigão, L. M. A.; Beton, P. H.; Champness, N. R. Tailoring Pores for Guest Entrapment in a Unimolecular Surface Self-Assembled Hydrogen Bonded Network. *Chem. Commun.* **2010**, *46*, 2775–2777.

(42) Räisänen, M. T.; Slater (née Phillips), A. G.; Champness, N. R.; Buck, M. Effects of Pore Modification on the Templating of Guest Molecules in a 2D Honeycomb Network. *Chem. Sci.* **2012**, *3*, 84–92.

(43) Berdunov, N.; Pollard, A. J.; Beton, P. H. Dynamic Scanning Probe Microscopy of Adsorbed Molecules on Graphite. *Appl. Phys. Lett.* **2009**, *94*, 043110.

(44) Madueno, R.; Räisänen, M. T.; Silien, C.; Buck, M. Functionalizing Hydrogen-Bonded Surface Networks with Self-Assembled Monolayers. *Nature* **2008**, *454*, 618–621.

(45) Theobald, J. A.; Oxtoby, N. S.; Champness, N. R.; Beton, P. H.; Dennis, T. J. S. Growth Induced Transitions between Fullerene Nanophases on a Self Assembled Molecular Framework. *Langmuir* **2005**, *21*, 2038–2041.

(46) Silly, F.; Shaw, A. Q.; Porfyrakis, K.; Warner, J. H.; Watt, A. A. R.; Castell, M. R.; Umemoto, H.; Akachi, T.; Shinohara, H.; Briggs, G. A. D. Grating of Single Lu@C$_{82}$ Molecules Using Supramolecular Network. *Chem. Commun.* **2008**, 4616–4618.

(47) Perdigão, L. M. A.; Staniec, P. A.; Champness, N. R.; Beton, P. H. Entrapment of Decanethiol in a Hydrogen-Bonded Bimolecular Template. *Langmuir* **2009**, *25*, 2278–2281.

(48) Saywell, A.; Magnano, G.; Satterley, C. J.; Perdigão, L. M. A.; Champness, N. R.; Beton, P. H.; O'Shea, J. N. Electrospray Deposition of C$_{60}$ on a Hydrogen-Bonded Supramolecular Network. *J. Phys. Chem. C* **2008**, *112*, 7706–7709.

(49) Saywell, A.; Magnano, G.; Satterley, C. J.; Perdigão, L. M. A.; Britton, A. J.; Taleb, N.; Giménez-López, M. C.; Champness, N. R.; O'Shea, J. N.; Beton, P. H. Self-Assembled Aggregates Formed by

3426

dx.doi.org/10.1021/ar5001378 | *Acc. Chem. Res.* 2014, 47, 3417–3427

Single Molecule Magnets on a Gold Surface. *Nat. Commun.* **2010**, *1*, 75.

(50) Wasio, N. A.; Quardokus, R. C.; Forrest, R. P.; Lent, C. S.; Corcelli, S. A.; Christie, J. A.; Henderson, K. W.; Kandel, S. A. Self-Assembly of Hydrogen-Bonded Two-Dimensional Quasicrystals. *Nature* **2014**, *507*, 86−89.